GLOBAL CORRELATION OF TOPOGRAPHIC HEIGHTS AND GRAVITY ANOMALIES

M. C. ROUFOSSE

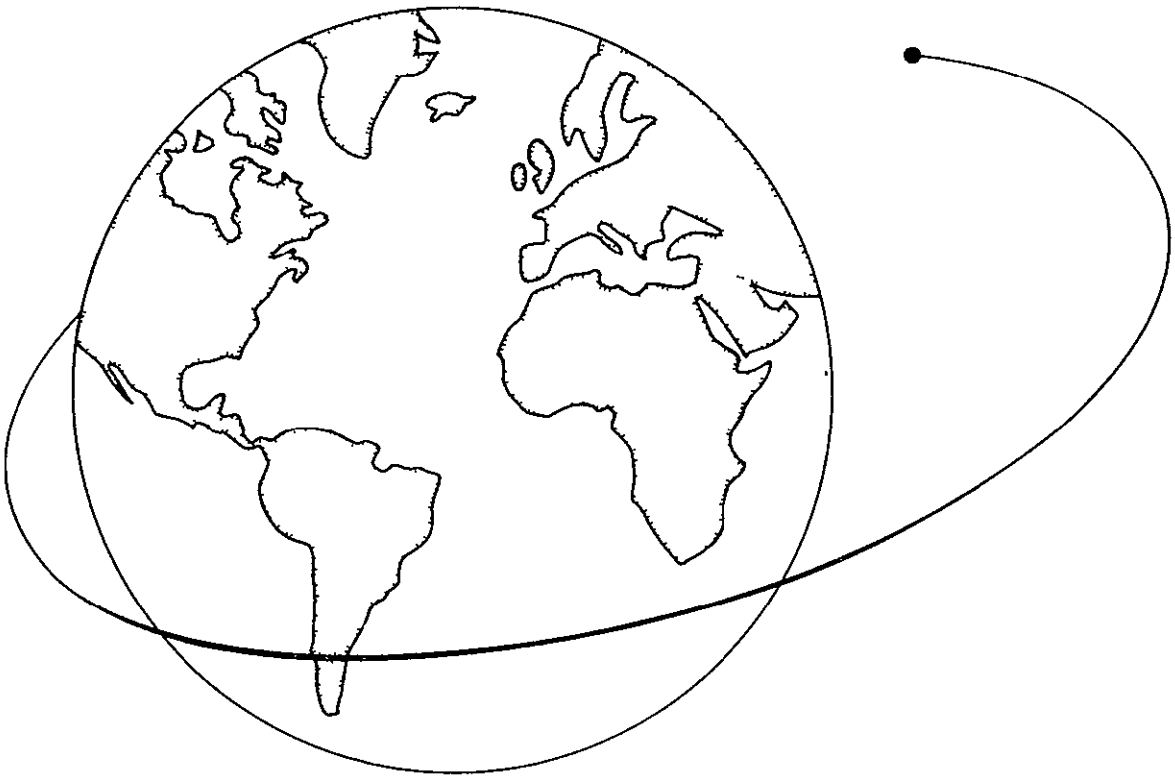

Smithsonian Astrophysical Observatory
SPECIAL REPORT 378

Research in Space Science
SAO Special Report No. 378

GLOBAL CORRELATION OF TOPOGRAPHIC HEIGHTS AND GRAVITY ANOMALIES

M. C. Roufosse

May 24, 1977

Smithsonian Institution
Astrophysical Observatory
Cambridge, Massachusetts 02138

TABLE OF CONTENTS

ILLUSTRATIONS

ILLUSTRATIONS (Cont.)

TABLES

ABSTRACT

The object of this research is to study and compare, on a worldwide scale, the short-wavelength features of the earth's gravity and topographic fields to determine whether any relationship exists between them. The short-wavelength features were obtained by subtracting a calculated 24th-degree-and-order field from observed data written in $1^\circ \times 1^\circ$ squares. The correlation between the two residual fields was examined by a program of linear regression. When run on a worldwide scale over oceans and continents separately, the program did not exhibit any correlation; this can be explained by the fact that the worldwide autocorrelation function for residual gravity anomalies falls off much faster as a function of distance than does that for residual topographic heights. The situation was different when the program was used in restricted areas, of the order of $5^\circ \times 5^\circ$ square. For 30% of the world, fair-to-good correlations were observed, mostly over continents. The slopes of the regression lines are proportional to "apparent" densities, which offer a large spectrum of values that are being interpreted in terms of features in the upper mantle consistent with available heat-flow, gravity, and seismic data.

GLOBAL CORRELATION OF TOPOGRAPHIC HEIGHTS AND GRAVITY ANOMALIES

M. C. Roufosse

1. INTRODUCTION

The theory of plate tectonics, in its present form, has been developed simultaneously by McKenzie and Parker (1967) and Morgan (1968). Their work provides a very successful kinematic theory of the present tectonic activity of the earth. Most of the available geophysical data can be explained by the postulate that the earth's surface is divided into a small number of rigid plates in relative motion with respect to each other, the relative motion between any two plates being described entirely by an angular-velocity vector. At midocean ridges, two plates move apart and material from the upper mantle upwells, cools, and creates new plates, while at ocean trenches, old plates are subducted and therefore destroyed. In order to ensure mass continuity, we must assume a return flow from trenches to ridges. This, then, describes large-scale convection, consisting of plates and return flows and therefore of horizontal dimensions governed by the dimensions of the plates themselves (i.e., several thousands of kilometers).

The relative motion between plates is what causes earthquakes. Earthquakes are apt to occur at trenches, where they reflect the forces at work in the subducted plates: extension when they are shallow and compression when they are deep. We also find shallow earthquakes at midplates; their origin is still uncertain, but some authors (see, e.g., McKenzie, 1972) associate them with the equalization of small displacement variations within one plate owing to its elasticity. The depth of a convection cell, on the other hand, is frequently

This work was supported in part by Grant NGR 09-015-002 from the National Aeronautics and Space Administration.

assumed to be on the order of 600 to 700 km, the depth of a seismic discontinuity. According to several observations (Birch, 1952; Anderson, 1967), a major phase change occurs at that depth. Experimental work suggests a rearrangement of the atoms surrounding silicon, resulting in a solid much stronger than spinel. McKenzie, Roberts, and Weiss (1974) assumed that under these circumstances, deformation would be much less likely to occur because of an increase in viscosity; there is, however, no evidence of such a viscosity change. A recent study by Jordan (1976) indicates that lithospheric slabs can penetrate into the lower mantle to a depth of 1000 km, below the 650-km discontinuity. At the present state of our knowledge, no definite limit can be placed on the depth of the convection cells.

The mechanism of large-scale convection adequately explains the energy released through earthquakes. However, it presents two difficulties: First, it is ineffective in transporting heat, and several authors (Sclater, Lawver, and Parsons, 1975; Richter and Parsons, 1975) claim that it cannot account for the observed high value of heat flow found in old oceanic basins. However, that observation has been criticized by Lister and Davis (1976) as lacking reliable heat-flow data and as containing in the available data a scatter larger than the effect studied. Schubert, Froidevaux, and Yuen (1976) have further proposed a viscous-dissipation model to account for these higher-than-expected values of heat flow. This debate is, in fact, extended to the model to be adopted: the boundary-layer model proposed by Turcotte and Oxburgh (1967) and defended by Davis and Lister (1974), versus the plate model proposed by Langseth, Le Pichon, and Ewing (1966) and refined by McKenzie (1967) and Sclater and Francheteau (1970). Knowing the value of heat flow in old oceanic regions is thus not going to resolve the ambiguity. Parsons and Sclater (1977) and Sclater and Parsons (1976) have offered more acceptable evidence to defend the plate model through bathymetry data. The oceanic depth, when plotted against age, clearly departs from the square-root-of-time law for ages larger than 70 m.y.

In this discussion, thermal conductivity has been neglected as a possible contributor to the observed heat-flow values. It was first believed (Clark, 1957) that the radiation component of thermal conductivity played a very impor-

tant role in transporting heat, increasing as the cube of temperature. This belief has been contested by Fukao (1969) and Fukao, Mizutani, and Uyeda (1968), who discovered an absorption peak due to iron (at 1 μ) in the olivine passband. According to their work, the absorption peak is very sensitive to temperature and could become so large at high temperatures that it would prevent radiation thermal conductivity from transferring heat effectively. This would leave only the contribution of the lattice thermal conductivity, studied by Schatz and Simmons (1972) and Roufosse and Klemens (1974). Lattice thermal conductivity initially decreases with increasing temperature, behaves as 1/T at moderately high temperatures, and then flattens progressively as the temperature increases further. The total thermal conductivity would therefore remain small and would be unable to explain the observed heat flow and the absence of extensive melting in the upper mantle. T. Shankland (1977, private communication), however, has questioned these findings: Recent studies by his group at Los Alomos (Nitsan, 1976) point toward larger values of the radiation thermal conductivity. Further work along that line is thus urgently needed to assess the exact role played by thermal conductivity.

The second difficulty of the large-scale convection theory is a question of stability. Several numerical and experimental models have been carried out by McKenzie et al. (1974), McKenzie and Weiss (1975), and Richter and Parsons (1975). Richter and Parsons show that two scales of convection are most likely present: a large-scale flow, related to plate motion and ordered over distances of several thousand kilometers, and a small-scale flow, featuring longitudinal rolls, which are 500 km in width and have their long axes aligned with the direction of plate motion.

Small-scale convection so far is only a working hypothesis, but one that conveniently explains the difficulties regarding the instability of large-scale convection and the higher-than-expected heat-flow values in old ocean basins. It is this subject that is of interest to us here. From the wealth of geophysical data on gravity anomalies and topographic heights currently available, we extract those portions that can be applied to mapping small-scale flow in the upper mantle. The pattern obtained will then be tested and further

refined by the use of seismic travel-time anomalies and heat-flow data where available. Our hope — and the object of our future research — is that a careful selection and combination of data will enhance our chances of discovering irrefutable traces of small-scale convection.

2. DESCRIPTION OF THE AVAILABLE DATA

The Smithsonian Astrophysical Observatory operates a geophysical data base that stores, among other quantities, observed free-air gravity anomalies written in 1° × 1° squares for approximately one-half of the whole world (37,405 data points), observed topographic heights written in 1° × 1° squares for the whole world (64,710 data points), and observed heat-flow data, where available, in 1° × 1° squares obtained from the Massachusetts Institute of Technology (6101 data points). In addition, from satellite and terrestrial data, the gravity field has now been computed complete through degree and order 24 (Gaposchkin and Lambeck, 1971; Gaposchkin, 1973, 1976). Similarly, a topographic-height field has been calculated by Lee and Kaula (1967) and revised by Balmino, Lambeck, and Kaula (1973) complete to degree and order 36. Finally, we have calculated a heat-flow field complete to degree and order 12 by using the coefficients published by Chapman and Pollack (1975).

The coefficients for the gravity, topographic-height, and heat-flow fields are all available in punched-card form. Programs have been written to compute these fields to any degree and order in 1° × 1° squares for the whole world, to average the data in 5° × 5° squares, and to contour the calculated field following any desired specifications.

3. THEORY GOVERNING THE USE OF AVAILABLE DATA

The aim of this research is to extract from these data all information that could be related to or indicative of small-scale convection in the upper mantle. It is therefore important, as a first step, to identify systematically the effects due to locally uncompensated or partially compensated topographic heights, these being likely large contributors to the free-air gravity anomalies. The next step will be to remove these effects where necessary.

Following the modified Vening-Meinesz model for isostasy, we shall assume regional compensation. Dorman and Lewis (1970) state that at short wavelengths, free-air anomalies are highly correlated with topography; the compensating masses are more remote, at a depth of 400 km or more (Lewis and Dorman, 1970), and will thus affect the long-wavelength features of the topography field. A field of degree and order higher than 24, corresponding to half-wavelengths shorter than 750 km, has been chosen in this work. In order to do so, we first calculated the topographic-height field in 1° × 1° squares for the whole world to degree and order 24 using the revised spherical-harmonics coefficients provided by Lee and Kaula (1967) and corrected by Balmino et al. (1973) and then removed that field from the corresponding file of 1° × 1° observed topographic heights for the whole world; we refer to the remaining file as residual topographic heights. The data are written in 1° × 1° squares, and each point is labeled according to whether it comes from a continental area or an oceanic area; oceanic data refer to points for which the topographic height is lower than 1000 m below sea level. We treated the gravity data in a similar manner: We removed a calculated field complete to degree and order 24 from the observed gravity data and refer to the remaining file as residual gravity anomalies.

The two residual files have been used for different purposes. First, in a statistical analysis, the covariance function, as a function of angular

distance separating pairs of points, has been obtained for both residual files. The results are given in Figure 1 for the residual gravity anomalies and in Figures 2 and 3 for residual topographic heights over oceans and over continents. It must be noted that since residual topographic heights present a stronger autocorrelation than do residual gravity anomalies, we cannot expect too good a correlation between residual gravity anomalies and residual topographic heights for the whole world.

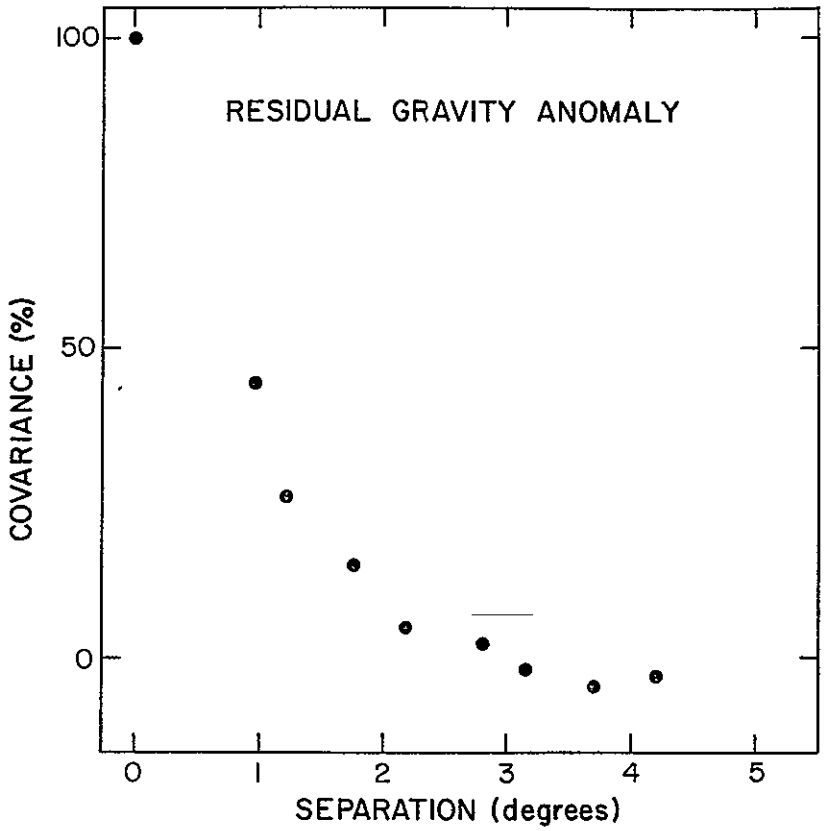

Figure 1. Covariance function for residual gravity anomalies.

Second, in an attempt to study the worldwide correlation between the two residual fields, we applied a linear-regression program for oceans and continents separately. As can be seen from Figures 4 and 5 and in Table 1, the correlation is poor; it is slightly better for continents than for oceans,

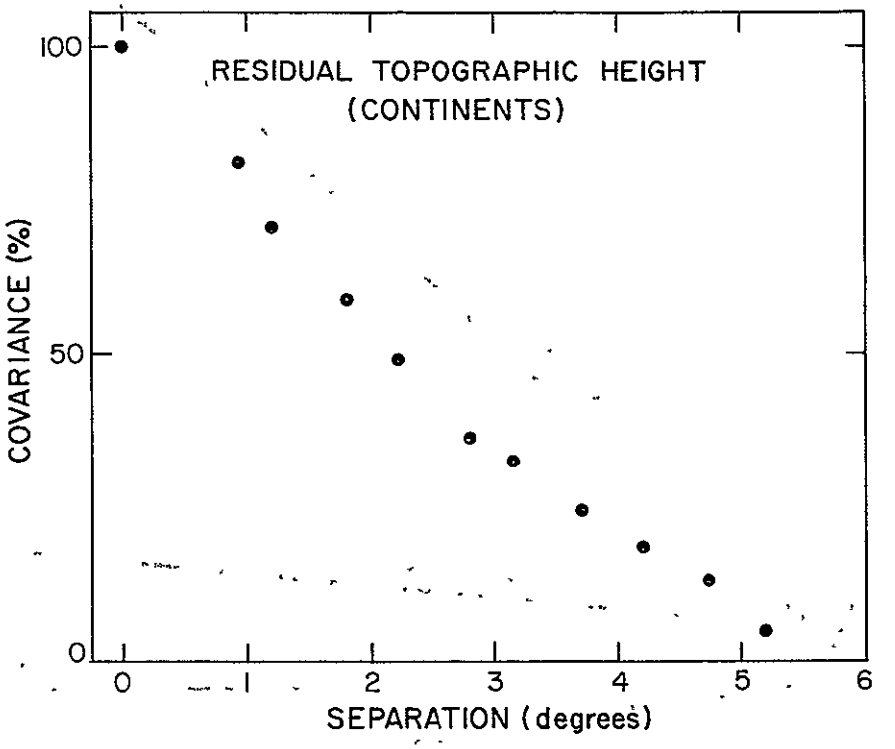

Figure 2. Covariance function for residual topographic heights over continents.

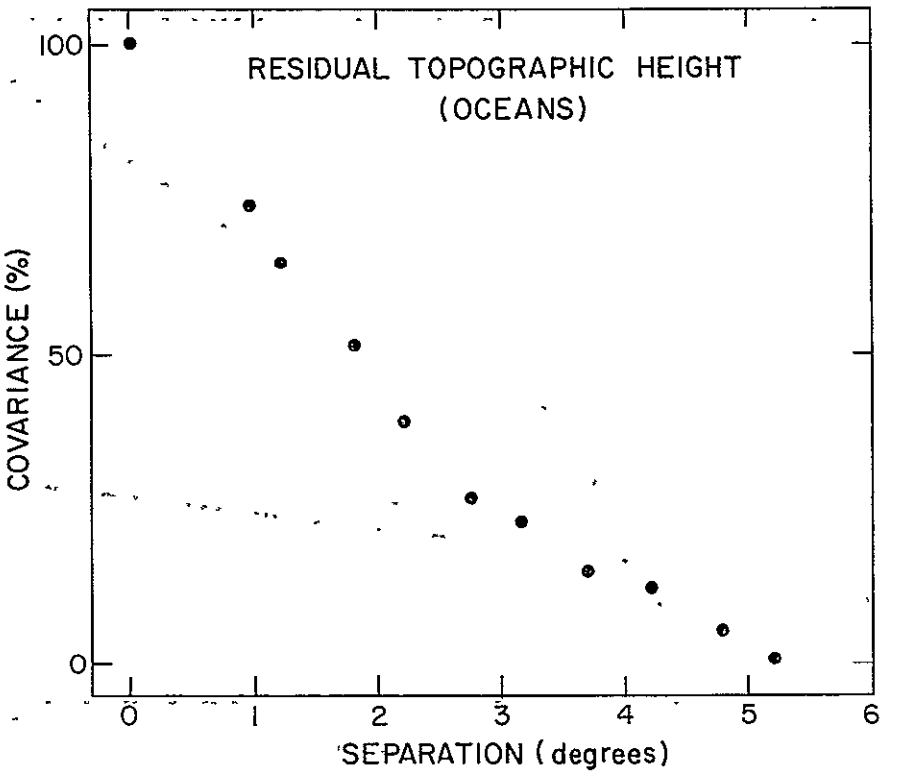

Figure 3. Covariance function for residual topographic heights over oceans.

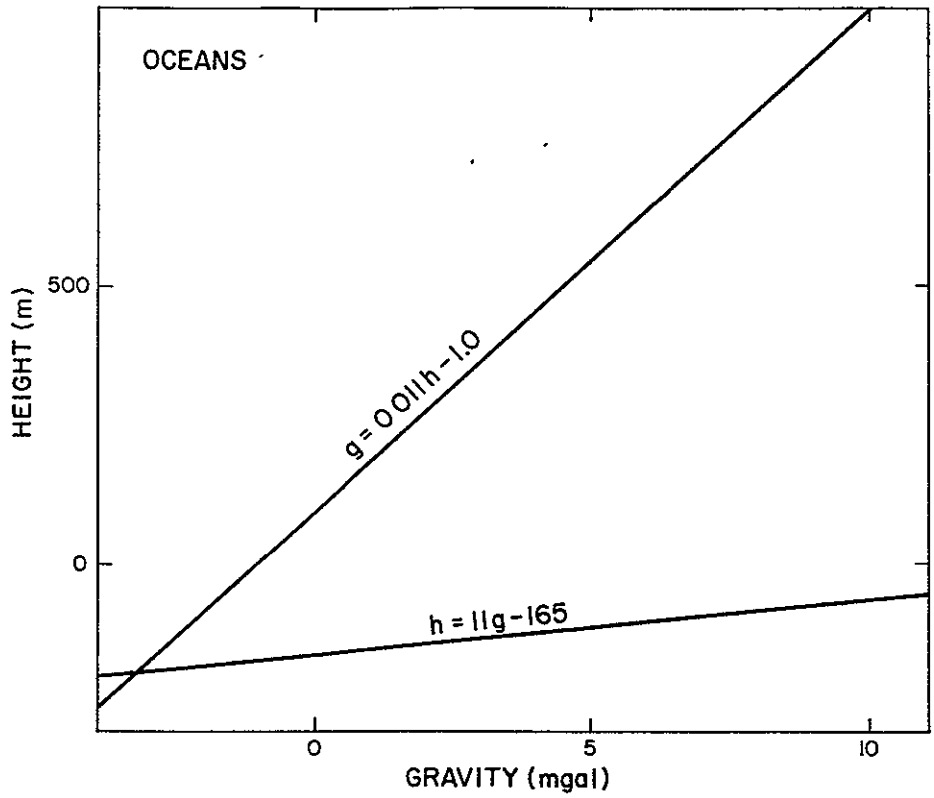

Figure 4. Linear-regression lines for oceans over the whole world.

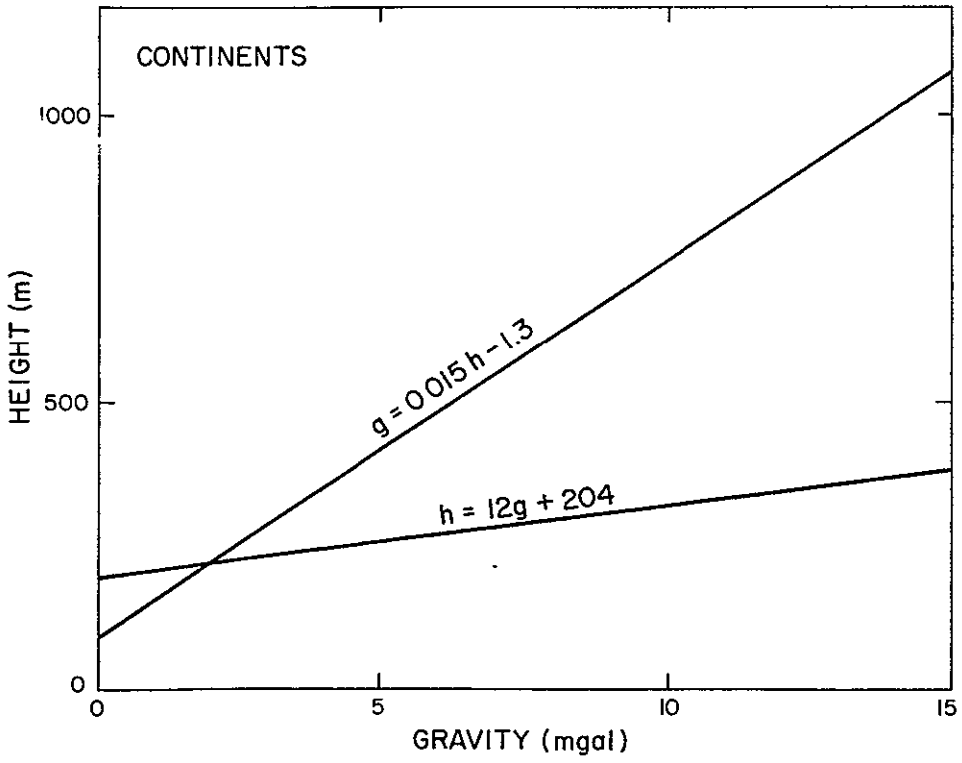

Figure 5. Linear-regression lines for continents over the whole world.

Table 1. Global correlation between residual topographic heights and residual gravity anomalies.

Parameter	Continents	Oceans
Correlation coefficient	0.43	0.34
Regression line	h = 12g + 204 m g = 0.015h - 1.3 mgal	h = 11g - 165 m g = 0.011h - 1.0 mgal
Slope	0.08 mgal/m 0.015 mgal/m	0.09 mgal/m 0.011 mgal/m
Mean residual gravity anomaly	2.21 mgal	-3.16 mgal
Mean residual topographic height	232 m	-199 m
Number of points	19813	17571
Root-mean-square gravity anomaly	24.6 mgal	24.8 mgal
Root-mean-square topographic height	703 m	776 m

the correlation coefficients being 0.4 and 0.3, respectively. We wish to point out that the linear-regression line giving topographic heights as a function of gravity anomalies is more reliable than is the regression line that gives the reverse, owing to the fact that residual gravity anomalies are "better behaved" statistical variables than are topographic heights. As seen in Figure 1, the autocorrelation curve of Δg as a function of distance falls off very rapidly, so that two points separated by a distance of 200 km can be considered independent variables. This is not the case for residual topographic heights, as shown in Figures 2 and 3. We also remark that the oceans are underrepresented, simply because fewer oceanic gravity data are available.

Mean densities of the regions studied can be determined from the slopes of the regression lines. We found mean-density values to be slightly lower for oceans than for continents; these values will be discussed later. As stated already, the correlation is poor, a result not unexpected. First, a comparison between the two covariance curves for residual topographic heights shows that these two fields behave differently and therefore cannot be expected to be related in a simple fashion. Furthermore, since the data cover

a wide range of tectonic features and ages, no unique relation can link the two fields. To avoid the latter problem, we studied small geographical regions on a systematic basis, dividing the world into 5° × 5° areas* and running the linear-regression program in each square where sufficient data (more than 13 points) were available. For each of these, we obtained both a linear-regression line whenever some correlation existed between the two sets of data and a brief description of the main tectonic features therein. The slope of each linear-regression line can be related to an "apparent density," which combines the real density with all other effects originating in the lithosphere and the upper mantle, such as the depths of the roots and thermal expansion. The global results are shown in Figure 6, where the mean apparent densities in 5° × 5° squares are superposed on continent tracings. Two representative 5° × 5° areas are shown in Figures 7 and 8 and in Tables 2 and 3. Statistical information on the goodness of the fit is shown in Table 4.

* It must be remarked that we are not dealing with regions of constant size; the area decreases with increasing latitude ϕ as $(\cos \phi)^2$.

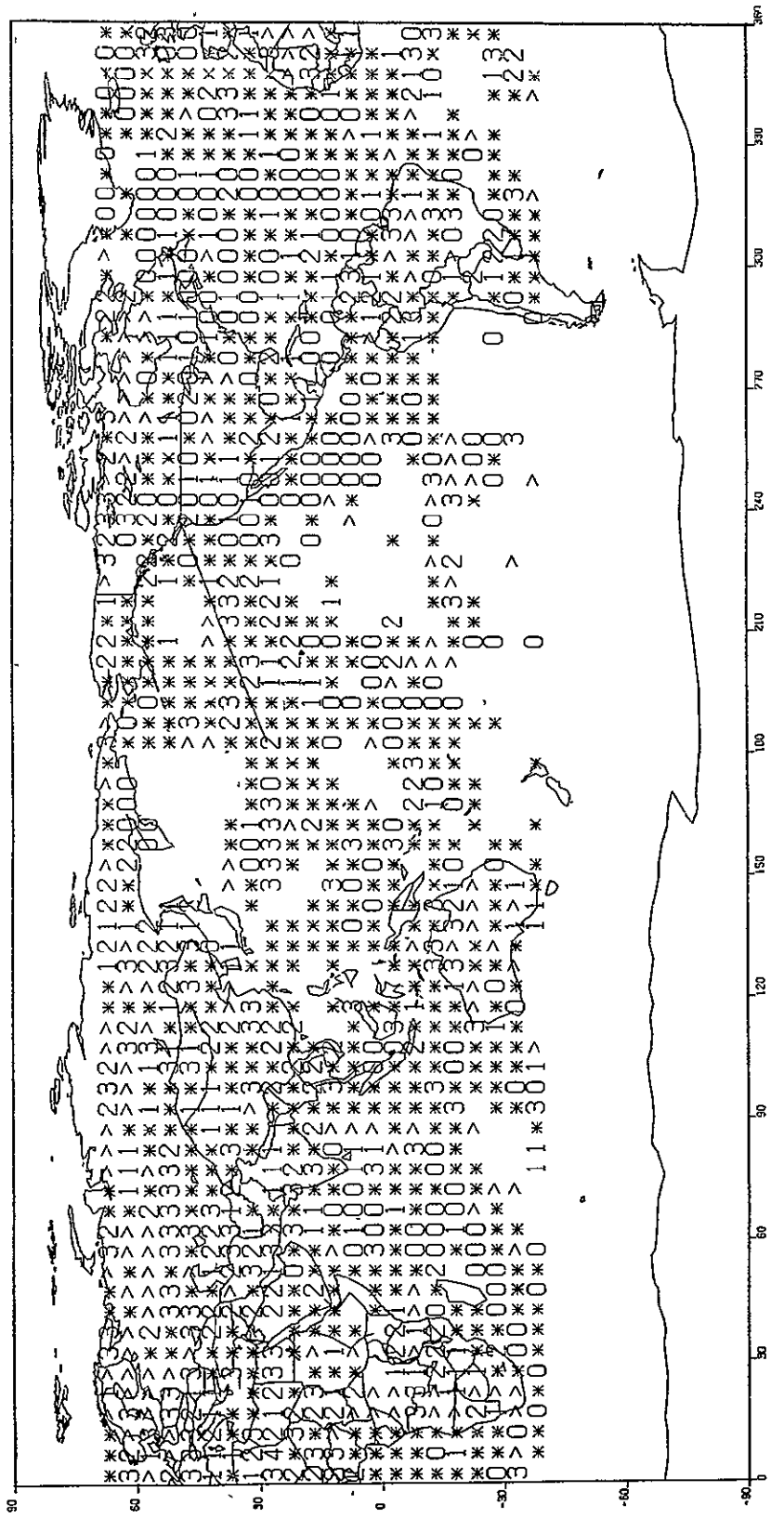

Figure 6. Values of apparent density in 5° × 5° squares for the whole world. Symbols: 0 = <1 g/cm^3, 1, 2, and 3 are the values of the slope in g/cm^3, > = >3 g/cm^3, and * = no correlation.

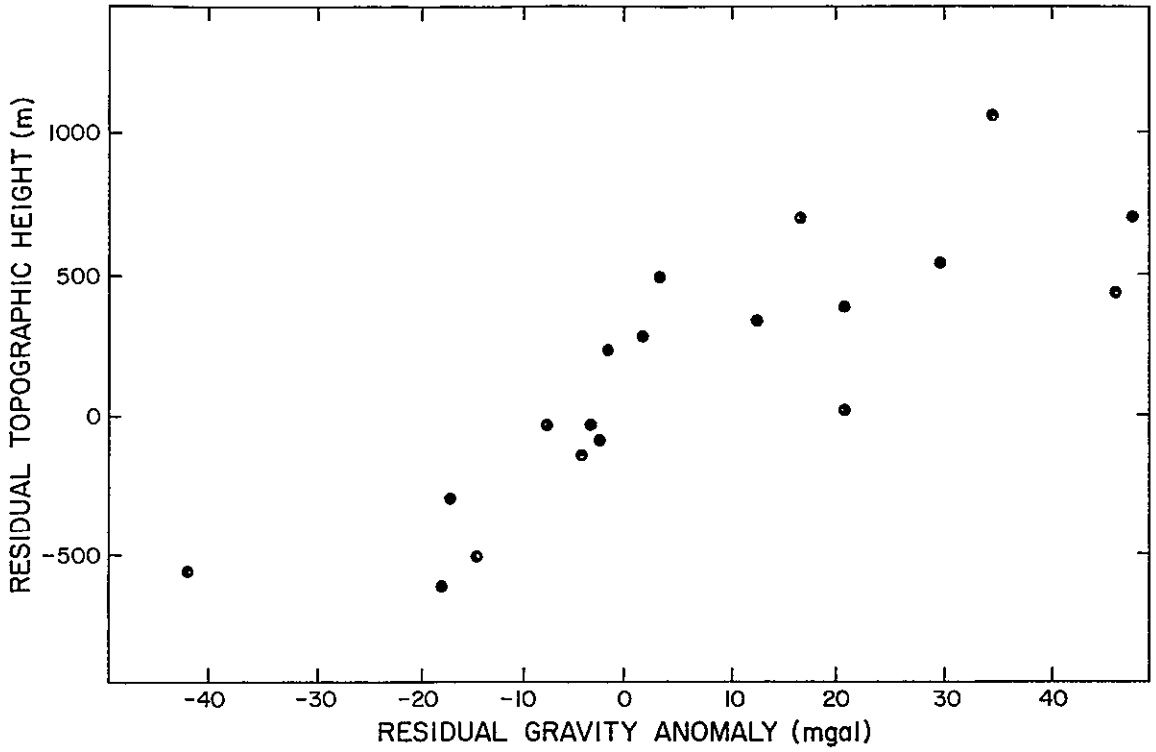

Figure 7. Plot of residual topographic heights versus residual gravity anomalies in the region between latitudes 45° and 40°N and longitudes 15° and 20°E.

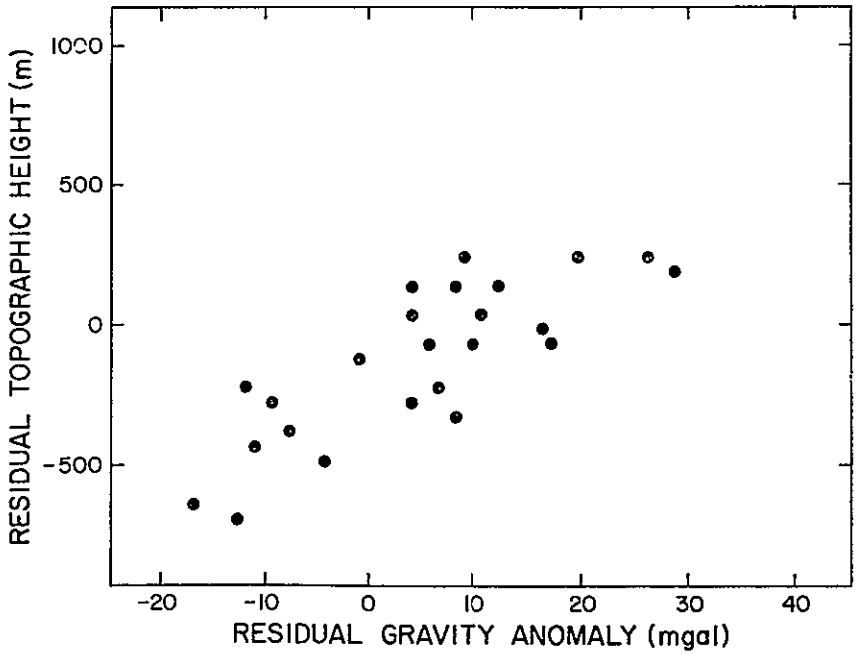

Figure 8. Plot of residual topographic heights versus residual gravity anomalies in the region between latitudes 45° and 40°N and longitudes 50° and 55°E.

Table 2. Residual topographic heights and residual gravity anomalies for the region between latitudes 45° and 40°N and longitudes 15° and 20°E.

Latitude	Longitude	Residual gravity anomaly (mgal)	Residual topographic height (m)
45°	16°	13.0	370
	17	-1.1	272
	18	-6.9	-10
	19	-16.3	-267
	20	-13.4	-450
44	16	-3.0	-2
	17	21.1	78
	18	48.6	736
	19	30.5	572
	20	3.8	532
43	16	-1.9	-60
	17	-41.5	-541
	18	-3.6	-83
	19	21.6	405
	20	17.1	757
42	16	47.3	448
	17	-16.9	-601
	18	-65.8	-502
	20	70.6	1105
41	16	35.5	1091
	17	52.6	435
	18	2.0	297

Table 3. Residual topographic heights and residual gravity anomalies for the region between latitudes 45° and 40°N and longitudes 50° and 55°E.

Latitude	Longitude	Residual gravity anomaly (mgal)	Residual topographic height (m)
45°	51°	7.2	-224
	52	10.5	-70
	53	16.8	8
	54	8.9	169
	55	20.0	266
44	51	9.1	-322
	52	18.2	-50
	53	11.2	41
	54	13.0	165
	55	26.7	254
43	51	-4.0	-492
	52	4.6	-249
	53	6.1	-63
	54	4.5	157
	55	9.7	263
42	51	-16.0	-619
	52	-7.0	-368
	53	-11.1	-236
	54	4.7	31
	55	29.2	233
41	51	-12.3	-703
	52	-10.1	-444
	53	-9.0	-246
	54	-0.2	-110
	55	58.5	14

Table 4. Statistical information derived from the plots in Figures 7 and 8 and the listings in Tables 2 and 3.

Region	Latitude 40° to 45°N, longitude 15° to 20°E	Latitude 40° to 45°N, longitude 50° to 55°E
Regression equations	$g = 5.3 \times 10^{-2}h - 2.3$ mgal $h = 13.3g + 91$ m	$g = 3.8 \times 10^{-2}h + 11.5$ mgal $h = 11.6g - 192$ m
Standard deviation	$\sigma_g = 16.5$ mgal $\sigma_h = 260.6$ m	$\sigma_g = 11.7$ mgal $\sigma_h = 204.3$ m
$\overline{g} = \frac{1}{n}\sum_{i=1}^{n} g_i$	8 mgal	7.6 mgal
$\overline{g^2} = \frac{1}{n}\sum_{i=1}^{n} g_i^2$	1.04×10^3 mgal^2	3.04×10^2 mgal^2
$\overline{h} = \frac{1}{n}\sum_{i=1}^{n} h_i$	2.08×10^2 m	-1.04×10^2 m
$\overline{h^2} = \frac{1}{n}\sum_{i=1}^{n} h_i^2$	2.8×10^5 m^2	8.6×10^4 m^2
Correlation coefficient	0.85	0.7
Covariance	1.27×10^4	2.87×10^3

4. CORRELATIONS OBSERVED OVER CONTINENTS

4.1 Introduction

So far, little global work has been done on the continents, although coverage of continental data is far better than that of oceanic data, for both topographic heights and gravity anomalies. Continental rocks contain more silica and are, therefore, less dense and unable to sink into the mantle. Oceanic crust, on the other hand, is denser and thus sinks easily through the mantle. As a consequence, the rocks that comprise continents are older than those in the oceanic crust, and we therefore expect continents to be more deformed and anomalous. We indeed find very different behavior from one region to another, as can be seen from Figure 6. We present below a description of the correlations observed for each continent separately.

4.2 Europe

In Europe, the correlations between residual gravity anomalies and topographic heights are generally very good. Over the northern part of Europe, the linear-regression lines exhibit slopes consistent with apparent densities on the order of 2.7 g/cm^3, or 0.1 mgal/m. The correlations are better in the west than they are in the east; the west consists principally of younger platforms, compared with the old platforms, covered with sediments, found in the east.

The slopes of the linear-regression lines for the southern part of Europe are consistent with apparent densities on the order of 1.5 g/cm^3 (0.06 mgal/m). This region corresponds to an Alpine foldbelt. The low apparent densities in this case can be explained by the following simplistic argument: In the presence of full isostatic compensation, a gravity anomaly, and hence its apparent density, will be equal to zero. If the apparent

density is not zero, we can assume that it is due to a lack of regional isostatic compensation and can use the equation

$$2\pi\gamma\rho_c h - 2\pi\gamma\Delta\rho r = 2\pi\gamma\rho_{ap} h \quad ,$$

where γ is the gravitational constant, ρ_c is the crustal density (= 2.7 g/cm^3), $\Delta\rho$ is the density contrast between the mantle and the crust (= 0.6 g/cm^3), ρ_{ap} is the apparent density derived from the linear-regression line, h is the topographic height, and r is the root dimension. Replacing all the quantities by the above values, we find that r is one-half that expected for a normal case of full isostatic compensation. This supports Bullard and Cooper's (1948) conclusion that some part of the light compensatory material is unusually shallow. Parker (1975) also came to the same conclusion, although he used different and more rigorous arguments.

4.3 Asia

No simple classification seems possible in Asia. As a rule, the entire northern part offers a better correlation between residual heights and residual gravity anomalies than does the south. The northwest, which corresponds to the Permian period, exhibits correlations with very large slopes and hence very large apparent densities, reflecting the presence of very little relief and large residual gravity anomalies. The source of these large gravity anomalies has not yet been determined. The north-central part, between the rivers Yenisey and Lena, corresponds to a region of Precambrian shield covered with sediment. Very few correlations between topographic heights and gravity anomalies are seen therein, and they do not exhibit any picture or trend.

East of the river Lena, the northeast area of Asia corresponds mostly to Mesozoic foldbelts with some Alpine folding toward the southeast (Kamchatka). The correlations there are good. In the Alpine area, we find a very small slope, or a very low value of apparent density, thus indicating full isostatic

compensation. In the Mesozoic foldbelt, correlations occur with higher apparent densities, of the order of 2.6 g/cm^3 (0.1 mgal/m).

In southern Asia, few areas show good correlations. A small region south of the Caspian Sea, which corresponds to an Alpine foldbelt, is characterized by apparent densities on the order of 2 g/cm^3 (0.08 mgal/m). To the east of the Caspian Sea, in a Hercynian region, the slope of the linear-regression line gives an apparent density of 2.7 g/cm^3 (0.1 mgal/m).

Scattered and occasional good correlations were found over the rest of the continent, but they could not be associated with any defined periods or tectonic schemes.

4.4 Africa

As a rule, we can associate good correlations in Africa with Precambrian shields covered with sediments. These regions generally show very little residual topographic height and large residual gravity anomalies. This effect is particularly marked in central Africa in the region where there is a large known negative gravity anomaly and lower-than-average heat flow.

The principal tectonic feature in the extreme northwestern part of Africa is Hercynian orogenesis, except for a narrow region of Alpine folding along the Mediterranean coast. The correlations in this area are good, with low values of apparent density (1.5 g/cm^3, or 0.06 mgal/m). The western region of South Africa, in a zone of recent Alpine activation on Precambrian basement, offers good correlations with low apparent densities.

The rest of Africa is mostly characterized by Precambrian shields. No systematic correlations are found in these areas.

4.5 North America

Only the western part of North America shows good correlations. This area corresponds roughly to Alpine and Mesozoic folded zones, while the central

and eastern regions are associated with the Precambrian period. The main characteristics of the western part of North America are a high heat flow, small residual gravity anomalies, and large residual topographic heights. These three features lead to low apparent densities, ranging from 0.5 to 1.5 g/cm^3 (0.02 to 0.06 mgal/m). The eastern portion of North America is Precambrian. It offers correlations with a wide spectrum of slopes and a small correlation coefficient.

4.6 South America

The data in South America are not very abundant, and we have been unable to detect any large areas with good correlations. Some reasonable regression lines are found in the extreme northern part, associated with an Alpine folded zone. On the average, the slopes indicate an apparent density of 1.5 g/cm^3 (0.06 mgal/m).

One region in central South America is characterized by a large horizontal gravity gradient. The variations of residual gravity anomalies there are very large and are followed by large variations in residual topographic heights. The two fields are quite anomalous in this area. The region consists of Precambrian shield exposed in some parts and covered with sediments in others and is characterized by a low value of the heat-flow field. The slope of the regression line leads to an apparent-density value of 2.7 g/cm^3 (0.14 mgal/m) or larger.

4.7 Australia

In Australia, the coastal areas offer correlations, but the slopes vary greatly. The apparent densities are generally lower on the eastern and southeastern sides of the island, which are mainly from the Permian period. The western part is mostly Precambrian.

4.8 Summary

In summary, several continental areas present good correlations between residual topographic heights and residual gravity anomalies. These areas are primarily associated with Alpine and Mesozoic folded zones; when this is the case, we also find low values of apparent density. Good linear-regression lines are also seen in regions associated with the Permian period. The apparent densities there are generally large, between 2 and 3 g/cm^3 (0.08 and 0.16 mgal/m).

5. CORRELATIONS OBSERVED OVER OCEANS

5.1 Introduction

The correlations between residual topographic heights and residual anomalies over the oceans have been studied extensively (Anderson, McKenzie, and Sclater, 1973; Watts, 1976; Watts and Talwani, 1974; Watts, Talwani, and Cochran, 1976; Cochran and Talwani, 1977; Sclater et al., 1975). However, these and other works do not use our definition of residual topographic height; for example, Sclater et al. (1975) define it as the observed bathymetry corrected for cooling and isostatic effects of sediment loading. The depth increase as a function of age has been calculated by Sclater, Anderson, and Bell (1971), Parker and Oldenburg (1973), and Davis and Lister (1974) by assuming a plate of infinite thickness. They found that the depth H increases with the square root of age,

$$\Delta H = \frac{2}{\pi^{1/2}} \alpha_{eff} T_i (kt)^{1/2} \quad ,$$

where α_{eff} is the effective thermal expansion coefficient, T_i the intrusion temperature, k the thermal diffusivity, and t the time. That law has been discussed and improved by Sclater et al. (1975) and Parsons and Sclater (1977), who took into account the finite thickness of the plate. Their new theory leads to a flattening of the $t^{1/2}$ curve for ages older than 80 m.y. and is in better agreement with the observed topographic data.

As can be seen from the scale on Figure 9 and from Figures 10 and 11, the cooling effect has been removed as a long-wavelength feature in our analysis, at least for plates that move faster than 1 cm/yr. Similarly, the residual gravity anomalies do not offer any definite trend as a function of distance to the ridge. This can be seen in Figures 12 through 17.

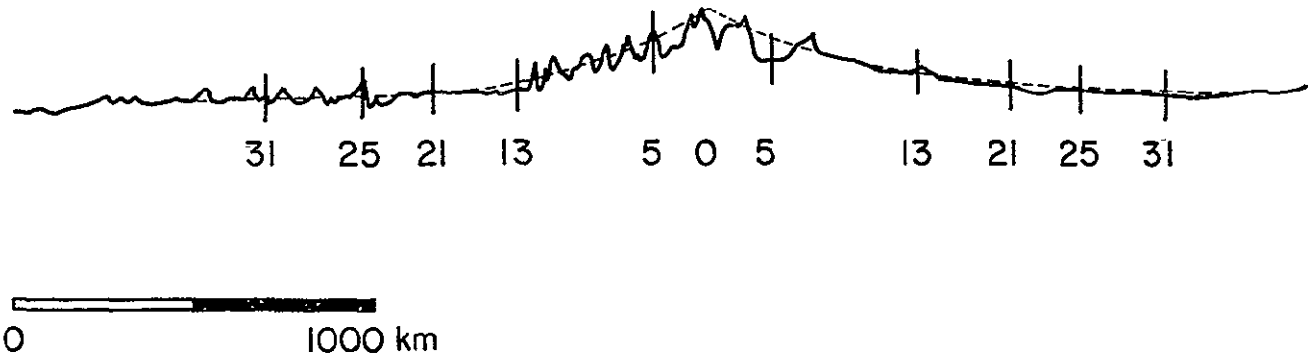

Figure 9. Profile of observed bathymetry across the mid-Atlantic ridge at 28°N.

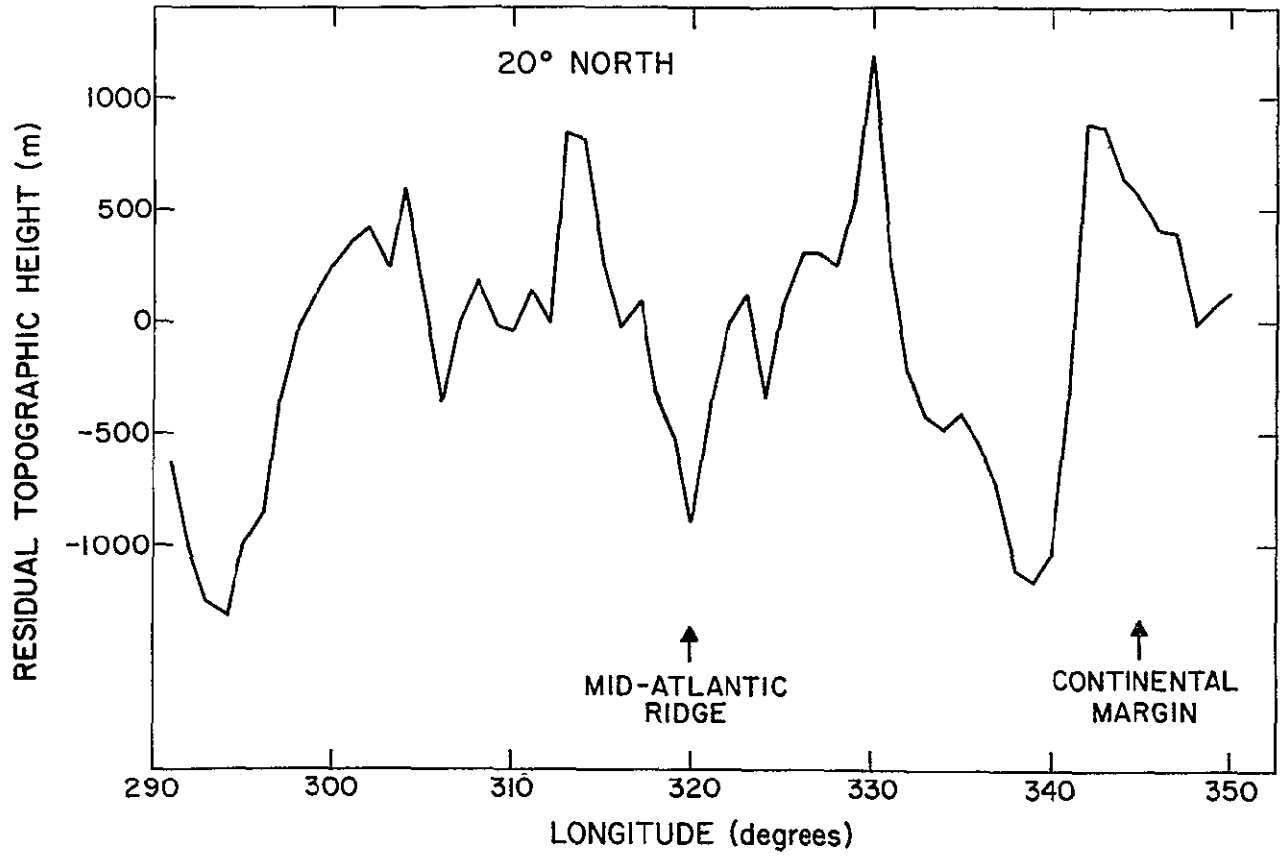

Figure 10. Profile of residual topographic heights across the mid-Atlantic ridge at latitude 20°N between longitudes 290° and 350°E.

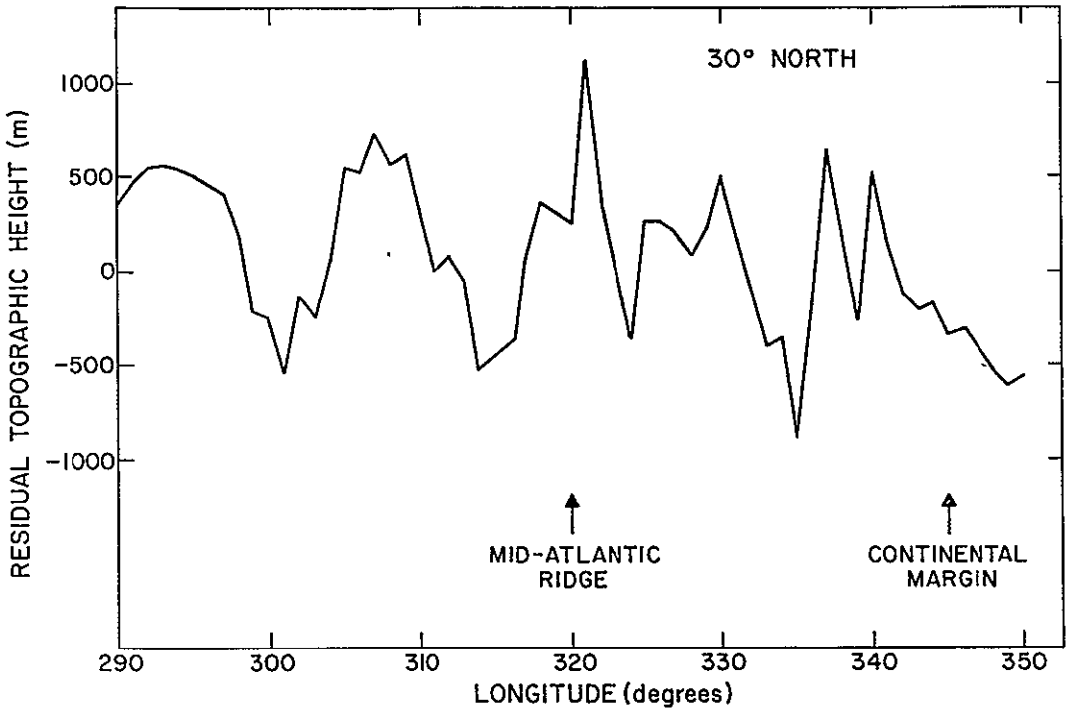

Figure 11. Profile of residual topographic heights across the mid-Atlantic ridge at latitude 30°N between longitudes 290° and 350°E.

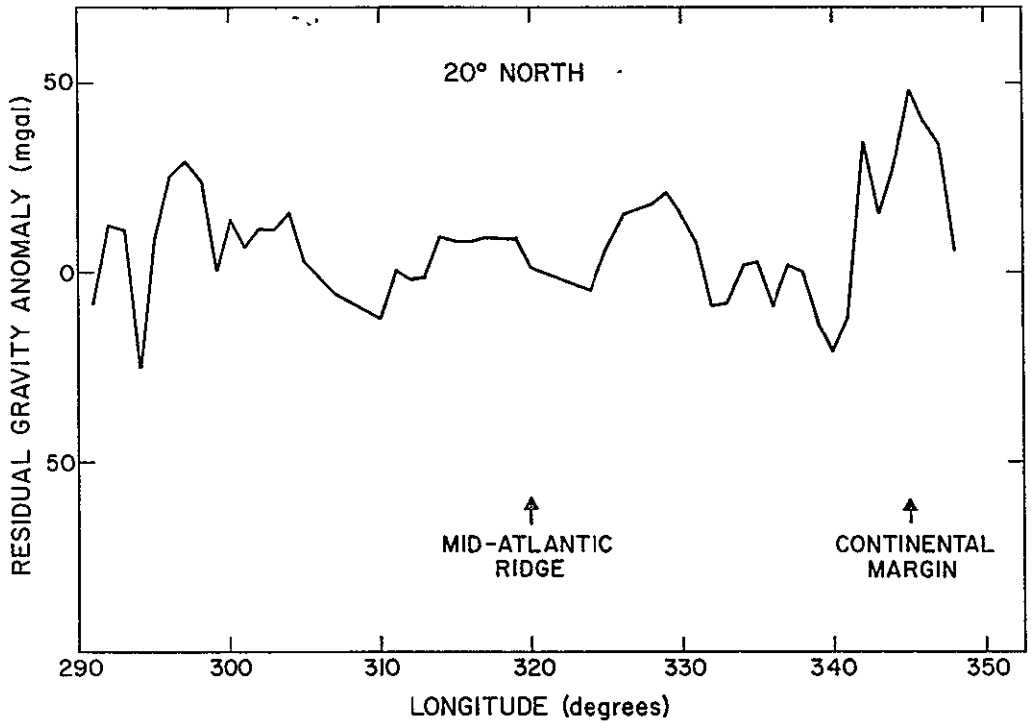

Figure 12. Profile of residual gravity anomalies across the mid-Atlantic ridge at latitude 20°N between longitudes 290° and 350°E.

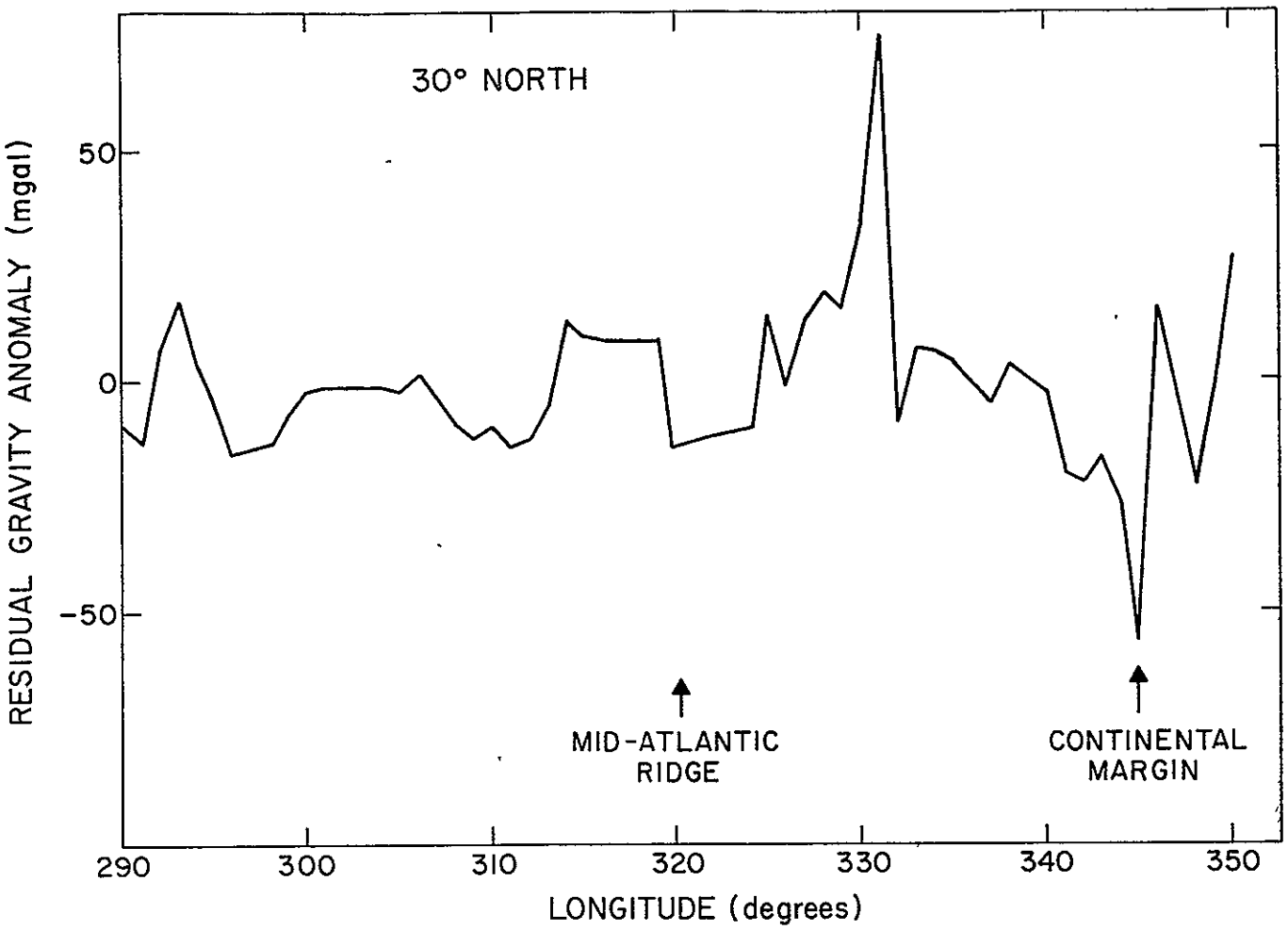

Figure 13. Profile of residual gravity anomalies across the mid-Atlantic ridge at latitude 30°N between longitudes 290° and 350°E.

Since, as mentioned previously, no large-scale correlations were discernible over the oceans, we shall thus proceed to describe those areas where regional correlations did occur and compare our results with those available in the literature.

5.2 Atlantic Ocean

In the Atlantic Ocean, we find a trend of good correlations following the mid-Atlantic ridge. The residual gravity-anomaly values vary little over the ridge, while the residual topographic heights reveal stronger variations. This leads to very low values of apparent density along the ridge axis, as can be seen in Figure 6.

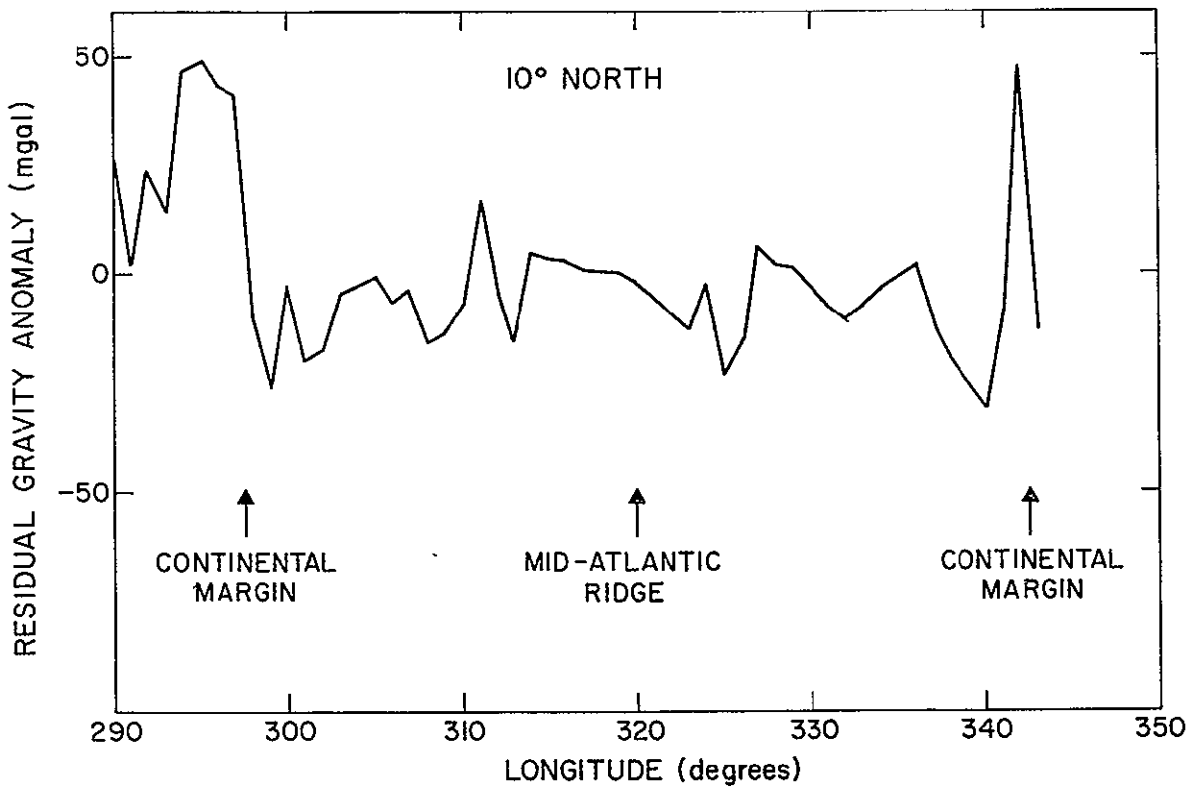

Figure 14. Profile of residual gravity anomalies across the Atlantic Ocean at latitude 10°N between longitudes 290° and 350°E.

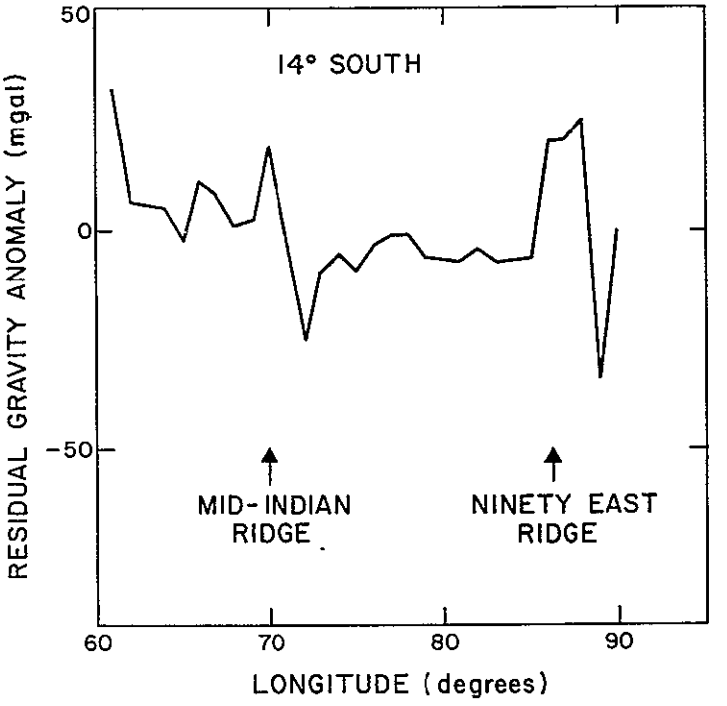

Figure 15. Profile of residual gravity anomalies across the Indian Ocean at latitude 14°S between longitudes 60° and 90°E.

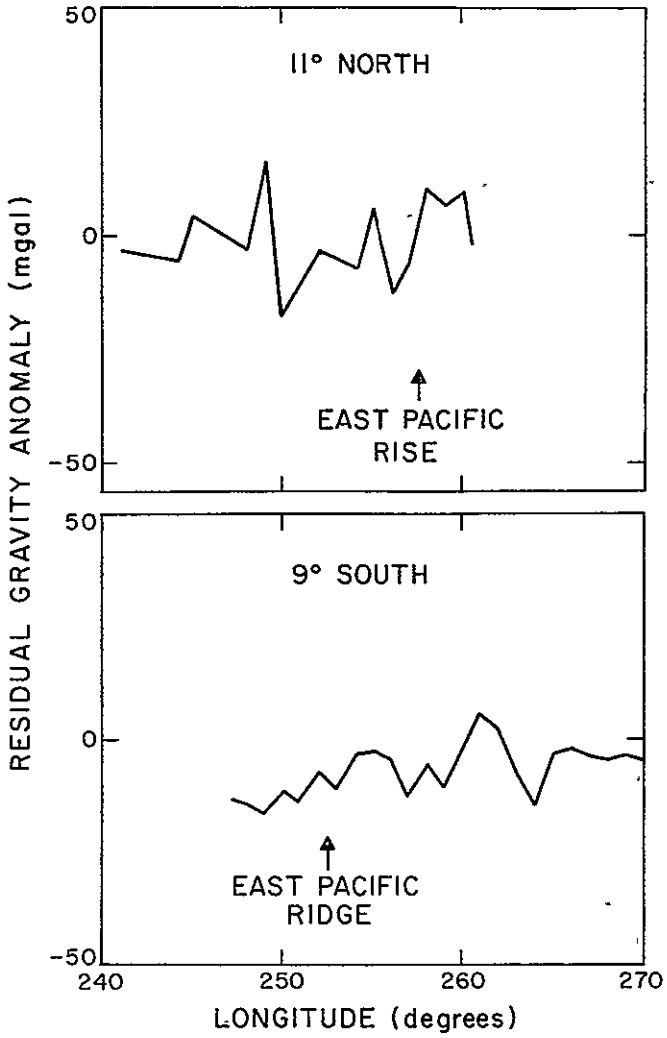

Figure 16. Profile of residual gravity anomalies across the Pacific Ocean at latitudes 11°N and 9°S between longitudes 240° and 270°E.

To the east of the mid-Atlantic ridge is another area exhibiting correlations, around the Azores, Canary Islands, and Cape Verde Islands. The apparent densities there are low, except in the vicinity of the Azores, where the apparent density is 2.5 g/cm^3 (0.1 mgal/m) and large residual gravity anomalies have been observed. This is a region of active volcanism, both submarine and on islands.

Correlations are also found in the northwestern Atlantic, near Bermuda Island, where we see low values of apparent density. Islands and some extinct

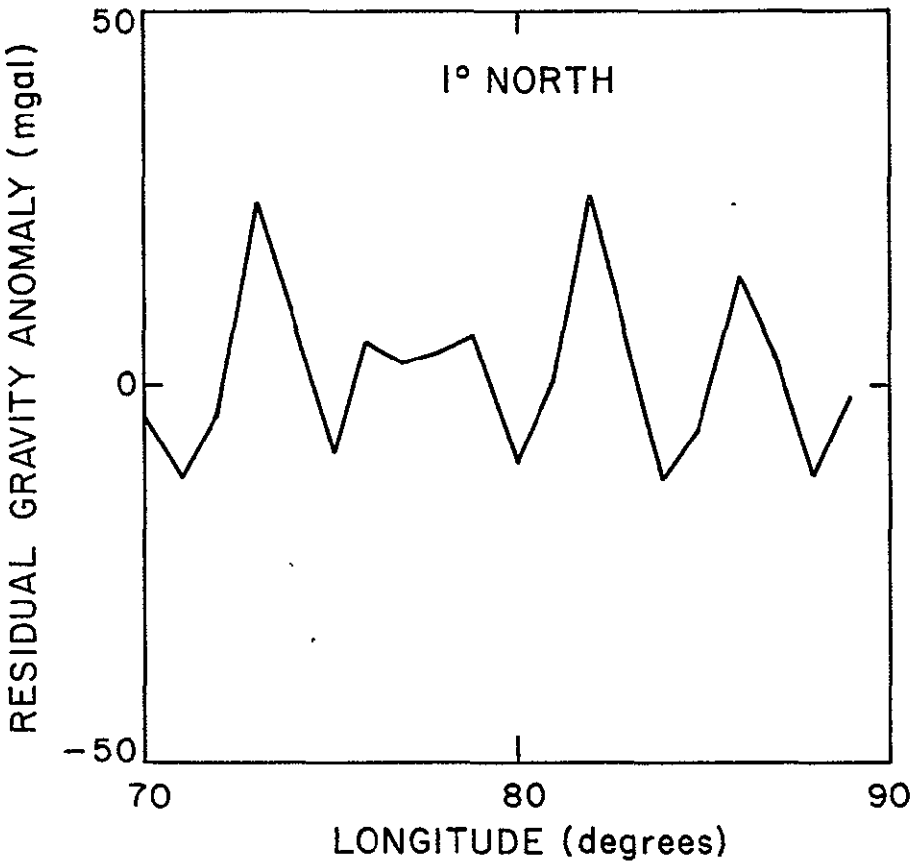

Figure 17. Profile of residual gravity anomalies across the Indian Ocean at latitude 1°N between longitudes 70° and 90°E.

submarine volcanoes comprise this area. Farther north in the Atlantic, Iceland offers a small region exhibiting good correlations of topographic heights with gravity anomalies.

Correlations in the vicinity of the Azores, Canary Islands, Bermuda, and Iceland have been reported in the literature by Sclater et al. (1975) and Cochran and Talwani (1977).

Near Fernando de Noronta, off the coast of Venezuela, we find a small area of good correlations associated with extinct volcanism.

Our data in the south Atlantic Ocean region are rather limited; apart from the mid-Atlantic ridge, little can be said about existing correlations. But along the mid-Atlantic ridge, where data are available, a well-defined correlation is accompanied by a low value of apparent density.

5.3 Pacific Ocean

Data in the Pacific Ocean are abundant in certain regions of interest and lacking in others. We have found correlations in the east-central part, in the area of the East Pacific rise, Cocos ridge, and Galapagos Islands. The residual gravity anomalies there are very small (see Figure 16), a fact reflected in low apparent-density values. This area is prolonged toward the south by the East Pacific ridge, which also offers fair-to-good correlations.

Another area of good correlations lies around Hawaii, where the residual gravity anomaly is quite variable, as seen in Figure 18. The major features

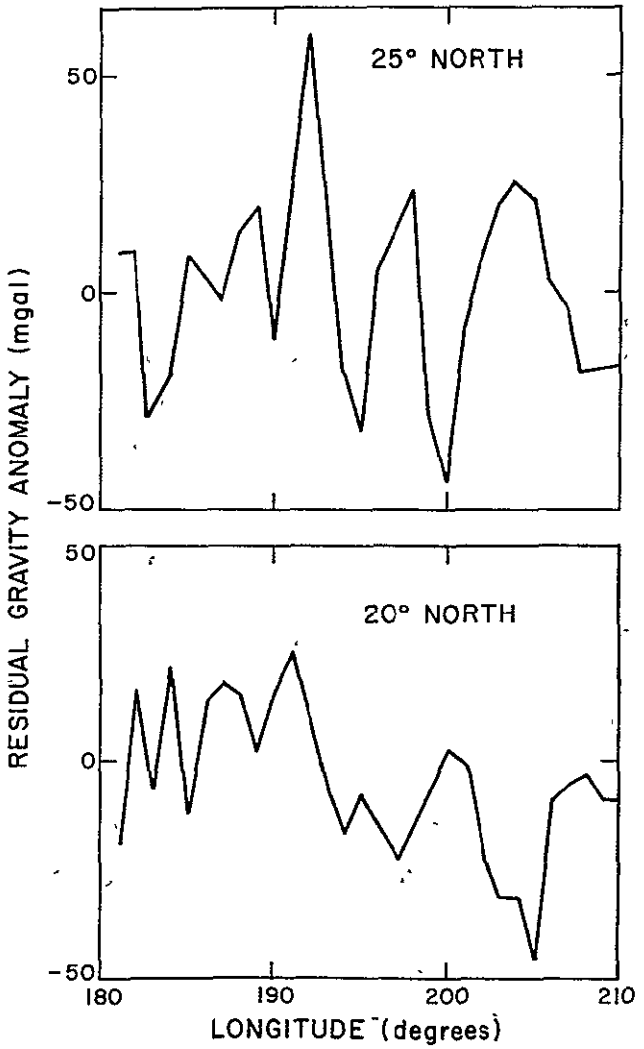

Figure 18. Profile of residual gravity anomalies across the Pacific Ocean at latitudes 25° and 20°N between longitudes 180° and 210°E.

of the residual gravity field are reflected in the residual topographic heights, but not perfectly (see Figure 19), as some features are blown up, while others are reduced. Along the trenches, we found no correlations at all. Both residual gravity-anomaly and residual topographic-height data vary greatly and independently.

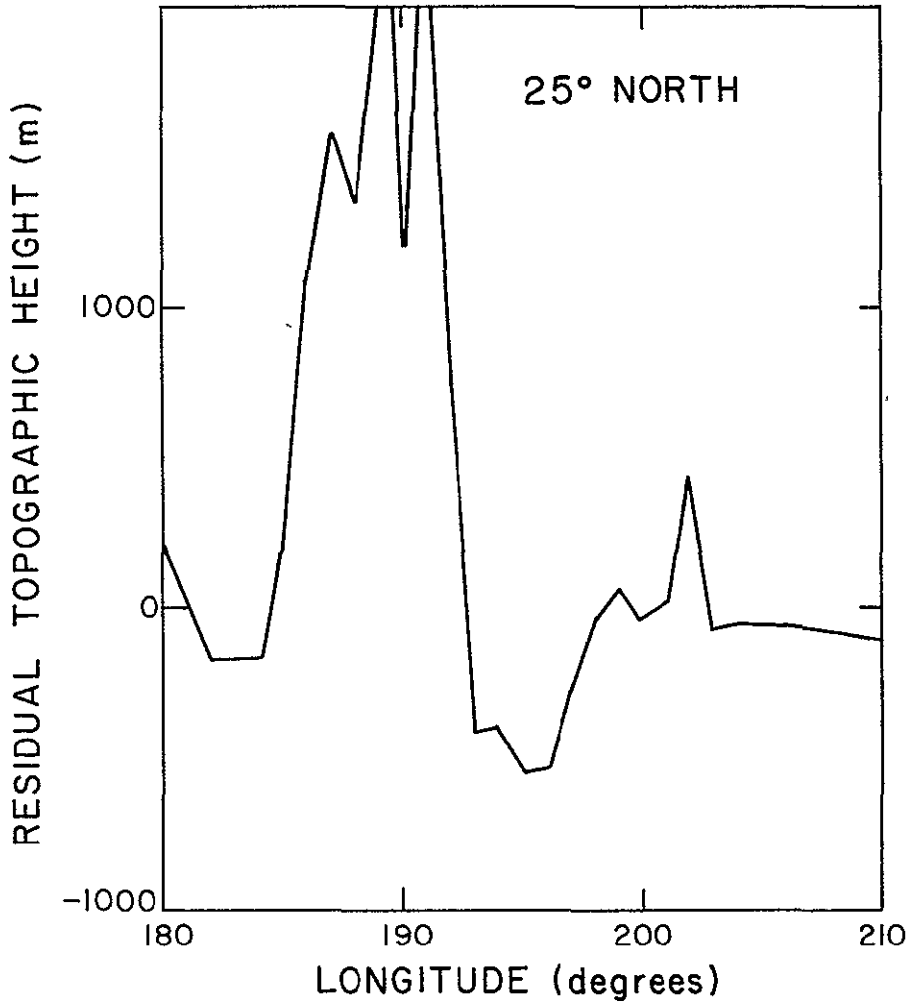

Figure 19. Profile of residual topographic heights across the Pacific Ocean at latitude 25°N between longitudes 180° and 210°E.

5.4 Indian Ocean

In the Indian Ocean, we found correlations in two areas exhibiting very different behavior. A correlation along the Carlsberg Ridge and the mid-Indian ridge axis seems to behave in the same manner as those found along the mid-Atlantic and mid-Pacific ridges. As shown in Figures 15 and 20, the

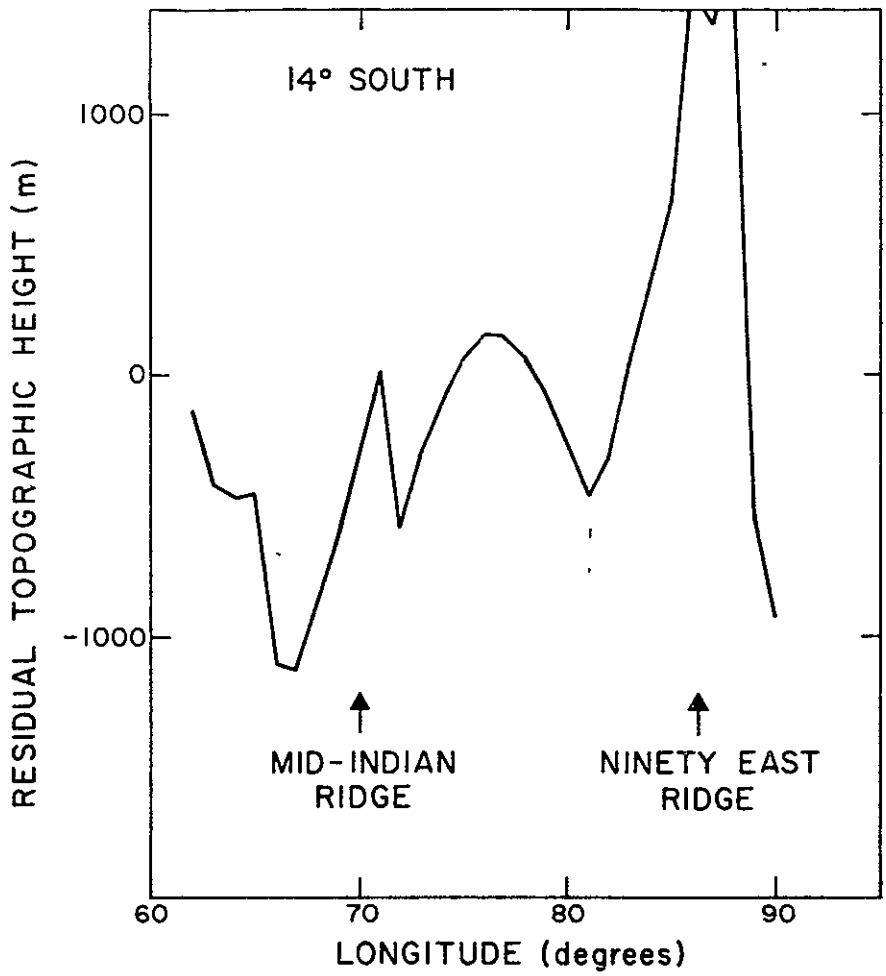

Figure 20. Profile of residual topographic heights across the Indian Ocean at latitude 14°S between longitudes 60° and 90°E.

major features in both fields coincide. They are less marked in the gravity field than in the topographic-height field, and we again find low values of apparent density. The other area lies south of India, close to a large negative gravity anomaly. In the residual gravity-anomaly file, the large negative trend has been removed as a long-wavelength feature and we are left with a variable field (Figure 17) whose major features are reflected in the residual topographic-height data. This leads to correlations with an apparent density larger than 2.5 g/cm^3, or a slope of 0.1 mgal/m.

A small area north of Madagascar, associated with volcanism, also shows correlations with very high apparent densities.

5.5 Summary

In summary, we find correlations over the oceans following most of the midocean ridges, in regions of recent or past volcanism, and over the large negative gravity anomalies south of India. So far, however, the gravity data over oceanic areas are quite limited. Furthermore, they are strongly biased because they have been chosen in "interesting" areas, which do not necessarily exhibit the behavior of typical oceanic regions. That we find correlations mostly along midoceanic ridges and in volcanic areas might simply be because these are the regions that have attracted most attention and for which better coverage is available.

6. DISCUSSION

Residual gravity anomalies as used in this study include only short-wavelength features. They must thus reflect either short-wavelength topographic features or some local density or temperature disturbances located in the lithosphere or upper mantle. In this work, we have identified and described those areas where residual anomalies in the gravity field are associated with uncompensated or partially compensated topographic heights. As a general rule, the regions where correlations occur over continents are associated with young orogenesis: Alpine and Mesozoic folded zones.

As mentioned previously, continental regions are generally quite anomalous; they are very old and were deformed through several consecutive processes (e.g., uplifts, foldings, erosion, glaciation, and postglacial rebound). Consequently, correlations occur in those areas where rocks have more recently been deformed or folded and where local imbalances might still exist. The older areas, which have not been activated through recent orogenesis, generally do not exhibit good correlations nor show any trends.

Most of the continental margins are good examples of full isostatic compensation. The residual gravity anomalies do not offer variations, while a strong transition is seen in the residual topographic heights.

For the oceans, the residual topographic heights correlate with the residual gravity anomalies along the ridges and in volcanic areas. For each of these, we have determined the slope of the regression line. We have written the slopes in terms of apparent densities, which lump all the factors influencing gravity anomalies.

The data are now ready for further interpretation, which we have just begun. Wherever a correlation is found between topographic heights and gravity anomalies, the trend has been removed in the hope of pinpointing within these

gravity-anomaly residues some features associated with small-scale convection in the mantle. In the Atlantic Ocean, where data are abundant, we have found a regular pattern along the profiles, paralleling the mid-Atlantic ridge (see Figure 21) with a wavelength of 500 km. Among other interpretations, such as transform faults or biased observed data, it could very well reveal traces of elongated rolls parallel to the direction of plate motion. According to Richter and Parsons (1975), small-scale convection is unlikely to have developed in the Atlantic Ocean owing to the small plate velocity. If it is present at all, it will exhibit a characteristic wavelength of 500 to 2000 km. We hope that future investigations will shed some light on this observation.

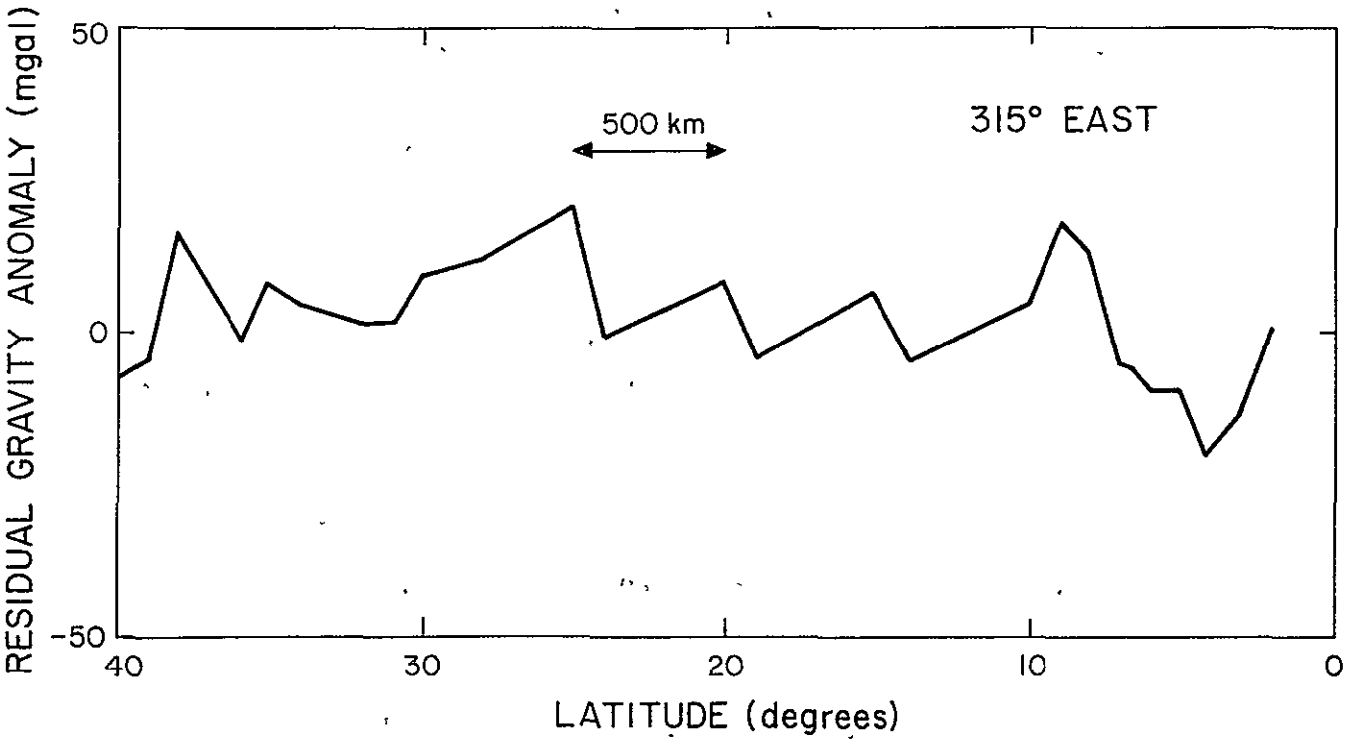

Figure 21. Profile of residual gravity anomalies parallel to the mid-Atlantic ridge at longitude 315°E between latitudes 0° and 40°N.

In a recent study, Marsh and Marsh (1976) used a calculated 13- to 22-degree gravity-anomaly field and discerned a long linear pattern of anomalies across the mid-Pacific area; these equidimensional features have a half-wavelength of 1000 km and an amplitude of ±4 to 8 mgal. Using a recent Smithsonian gravity-field determination (Gaposchkin, 1976) for degree and order 12 to 24, we have been unable to reproduce

these rolls. Nor did our residual gravity anomalies exhibit such features, probably because, in part, of an insufficient number of observed gravity anomalies in that area.

Along a similar line, Menard and Dorman (1976, 1977) found linear trends in the residual topographic heights in the Pacific Ocean, parallel to the direction of plate motion. Their residual topographic heights are further corrected for the effect of oceanic-depth anomalies as a function of latitude. Observing that the ridge crests are roughly 700 m deeper at the equator than at high latitudes, they removed that effect from the generally admitted residual topographic heights (see, for example, Sclater et al., 1975). The final residuals show linear features with wavelengths of 4000 km and vertical contrasts of 0.7 to 1.0 km. The general directional trend of this pattern is similar to that observed in the short-wavelength features of the gravity field calculated by Marsh and Marsh (1976), but the crest-to-crest distance is much larger; this latter distance is also much larger than the theoretical value of 500 km predicted by Richter and Parsons (1975).

It must be noted that the average slope found for the correlation lines over the midoceanic ridges is $3.3 \times 10^{-2} \pm 0.9 \times 10^{-2}$ mgal/m. This result is not inconsistent with theoretical values of the slopes calculated by McKenzie et al. (1974) on the basis of their convection model, which contains several simplifying assumptions: 1) convection limited to the upper 700 km; 2) newtonian fluid with constant viscosity, density, thermal-expansion coefficient, thermal conductivity, and heating rate; 3) periodic horizontal boundary conditions; and 4) two dimensions. The most important conclusion of that analysis is that over a rising flow, surface deformation dominates thermal expansion and therefore produces a positive gravity anomaly; this result is independent of the type of heating adopted (from below, from within, or a mixture of both), of the Rayleigh number, and of the aspect ratio of the confining box. Furthermore, a similar slope has been observed by Anderson et al. (1973) from data points collected along a 48100-km length of the worldwide ridge system.

Finally, we observed that when a correlation occurs, the slope of the regression line is generally larger for older tectonic features. That observation demands further investigation, and we intend to study the available data systematically to see whether we can discover a correlation between age and slope. This could reveal information on the time necessary to reach equilibrium and on the structure and time evolution of the lithosphere.

ACKNOWLEDGMENTS

I want to express my gratitude to Dr. E. M. Gaposchkin, who reviewed this manuscript and offered several helpful discussions and suggestions during the course of this research. I wish to thank Peggy Anderson for her assistance in the use of the geophysical data base and Cindy Wong for editing the manuscript.

REFERENCES

ANDERSON, D. L.

1967. Phase changes in the upper mantle. Science, vol. 157, pp. 1165-1173.

ANDERSON, R. N., McKENZIE, D. P., and SCLATER, J. G.

1973. Gravity, bathymetry and convection within the earth. Earth and Planet. Sci. Lett., vol. 18, pp. 391-407.

BALMINO, G., LAMBECK, K., and KAULA, W. M.

1973. A spherical harmonic analysis of the earth's topography. Journ. Geophys. Res., vol. 78, pp. 478-481.

BIRCH, F.

1952. Elasticity and constitution of the earth's interior. Journ. Geophys. Res., vol. 57, pp. 227-289.

BULLARD, E. C., and COOPER, R. I. B.

1948. The determination of the masses necessary to produce a given gravitational field. Proc. Roy. Soc. Lond., vol. A194, pp. 332-347.

CHAPMAN, D., and POLLACK, H. N.

1975. Global heat flow: A new look. Earth Planet. Sci. Lett., vol. 28, pp. 23-32.

CLARK, S. P.

1957. Radiative transfer in the earth's mantle. Trans. Amer. Geophys. Union, vol. 38, pp. 931-938.

COCHRAN, J. R., and TALWANI, M.

1977. Free-air gravity anomalies in the world's oceans and their relationship to residual elevation. Submitted to Geophys. Journ. Roy. Astron. Soc.

DAVIS, E. E., and LISTER, C. R. B.

1974. Fundamentals of ridge crest topography. Earth Planet. Sci. Lett., vol. 21, pp. 405-413.

DORMAN, L. M., and LEWIS, B. T. R.

1970. Experimental isostasy. 1. Theory of the determination of the earth's isostatic response to a concentrated load. Journ. Geophys. Res., vol. 75, pp. 3357-3365.

FUKAO, Y.

1969. On the radiative heat transfer and the thermal conductivity in the upper mantle. Bull. Earthquake Res. Inst., Tokyo Univ., vol. 47, pp. 549-569.

FUKAO, Y., MIZUTANI, H., and UYEDA, S.

1968. Optical absorption spectra at high temperatures and radiative thermal conductivity of olivines. Phys. Earth Planet. Interiors, vol. 1, pp. 57-62.

GAPOSCHKIN, E. M.

1973. 1973 Smithsonian Standard Earth (III) (editor). Smithsonian Astrophys. Obs. Spec. Rep. No. 353, 388 pp.

1976. Gravity-field determination using laser observations. Presented at The Royal Society Discussion Meeting, London, February; proceedings in press.

GAPOSCHKIN, E. M., and LAMBECK, K.

1971. The earth's gravity field to sixteenth degree and station coordinates from satellite and terrestrial data. Journ. Geophys. Res., vol. 76, pp. 4855-4883.

JORDAN, T.

1976. Lithospheric slab penetration into the lower mantle (abstract). Trans. Amer. Geophys. Union, vol. 57, p. 962.

LANGSETH, M. G., LE PICHON, X., and EWING, M.

1966. Crustal structure of midocean ridges. 5. Heat flow through the Atlantic Ocean floor and convection currents. Journ. Geophys. Res., vol. 71, pp. 5321-5355.

LEE, W. H. K., and KAULA, W. M.

1967. A spherical harmonic analysis of the earth's topography. Journ. Geophys. Res., vol. 72, pp. 753-758.

LEWIS, B. T. R., and DORMAN, L. M.

1970. Experimental isostasy. 2. An isostatic model for the U.S.A. derived from gravity and topography data. Journ. Geophys. Res., vol. 75, pp. 3367-3386.

LISTER, C. R. B., and DAVIS, E. E.

1976. Comments on "Comparison of long wavelength residual elevation and free air gravity anomalies in the North Atlantic and possible implications for the thickness of the lithospheric plate" by Sclater, Lawver, and Parsons. Journ. Geophys. Res., vol. 81, pp. 4957-4959.

MARSH, B. D., and MARSH, J. G.

1976. On global gravity anomalies and two scale mantle convection. Journ. Geophys. Res., vol. 81, pp. 5267-5280.

McKENZIE, D. P.

1967. Some remarks on heat flow and gravity anomalies. Journ. Geophys. Res., vol. 72, pp. 6261-6273.

1972. Plate tectonics. In The Nature of the Solid Earth, ed. by E. C. Robertson, McGraw-Hill Book Co., New York, pp. 323-360.

McKENZIE, D. P., and PARKER, R. L.

1967. The North Pacific: An example of tectonics on a sphere. Nature, vol. 216, pp. 1276-1280.

McKENZIE, D. P., ROBERTS, J. M., and WEISS, N. O.

1974. Convection in the earth's mantle: Towards a numerical simulation. Journ. Fluid Mech., vol. 62, pp. 465-538.

McKENZIE, D. P., and WEISS, N.

1975. Speculations on the thermal and tectonic history of the earth. Geophys. Journ. Roy. Astron. Soc., vol. 42, pp. 131-174.

MENARD, H. W., and DORMAN, L. M.

1976. On the variation of ocean depth with latitude (abstract). Trans. Amer. Geophys. Union, vol. 57, p. 933.

1977. Dependence of depth anomalies upon latitude and plate motion. In preparation.

MORGAN, W. J.

1968. Rises, trenches, great faults, and crustal blocks. Journ. Geophys. Res., vol. 73, pp. 1959-1982.

NITSAN, U.

1976. The effect of scattering on radiative heat transfer in the earth's mantle (abstract). Trans. Amer. Geophys. Union, vol. 57, p. 1005.

PARKER, R. L.

1975. The theory of ideal bodies for gravity interpretation. Geophys. Journ. Roy. Astron. Soc., vol. 42, pp. 315-334.

PARKER, R. L., and OLDENBURG, D. W.
1973. A thermal model for oceanic ridges. Nature, vol. 242, pp. 137-139.
PARSONS, B., and SCLATER, J. G.
1977. An analysis of the variation of ocean heat flow and depth with age. Journ. Geophys. Res., in press.
RICHTER, F. M., and PARSONS, B.
1975. On the interaction of two scales of convection in the mantle. Journ. Geophys. Res., vol. 80, pp. 2529-2541.
ROUFOSSE, M. C., and KLEMENS, P.
1974. Lattice thermal conductivity of minerals at high temperatures. Journ. Geophys. Res., vol. 79, pp. 703-705.
SCHATZ, J. F., and SIMMONS, G.
1972. Thermal conductivity of earth materials at high temperatures. Journ. Geophys. Res., vol. 77, pp. 6966-6983.
SCHUBERT, G., FROIDEVAUX, C., and YUEN, D. A.
1976. Oceanic lithosphere and asthenosphere: Thermal and mechanical structure. Journ. Geophys. Res., vol. 81, pp. 3525-3540.
SCLATER, J. G., ANDERSON, R. N., and BELL, M. L.
1971. The elevation of ridges and the evolution of the central eastern Pacific. Journ. Geophys. Res., vol. 76, pp. 7888-7915.
SCLATER, J. G., and FRANCHETEAU, J.
1970. The implications of terrestrial heat flow observations on current tectonic and geochemical models of the crust and upper mantle of the earth. Geophys. Journ. Roy. Astron. Soc., vol. 20, pp. 509-542.
SCLATER, J. G., LAWVER, L. A., and PARSONS, B.
1975. Comparison of long wavelength residual elevation and free air gravity anomalies in the North Atlantic and possible implications for the thickness of the lithospheric plate. Journ. Geophys. Res., vol. 80, pp. 1031-1052.
SCLATER, J. G., and PARSONS, B.
1976. Reply to Lister and Davis. Journ. Geophys. Res., vol. 81, pp. 4960-4964.
TURCOTTE, D. L., and OXBURGH, E. R.
1967. Finite amplitude convection cells and continental drift. Journ. Fluid Mech., vol. 28, pp. 29-42.

WATTS, A. B.

1976. Gravity and bathymetry in the central Pacific Ocean. Journ. Geophys. Res., vol. 81, pp. 1533-1553.

WATTS, A. B., and TALWANI, M.

1974. Gravity anomalies seaward of deep-sea trenches and their tectonic implications. Geophys. Journ. Roy. Astron. Soc., vol. 36, pp. 57-90.

WATTS, A. B., TALWANI, M., and COCHRAN, J. R.

1976. Gravity field of the northwest Pacific Ocean basin and its interior. In The Geophysics of the Pacific Ocean Basin and Its Margin, ed. by G. H. Sutton, M. H. Manghnani, and R. Moberly, AGU Geophys. Mono. 19, Washington, D.C., pp. 17-34.

NOTICE

This series of Special Reports was instituted under the supervision of Dr F. L. Whipple, Director of the Astrophysical Observatory of the Smithsonian Institution, shortly after the launching of the first artificial earth satellite on October 4, 1957. Contributions come from the Staff of the Observatory.

First issued to ensure the immediate dissemination of data for satellite tracking, the reports have continued to provide a rapid distribution of catalogs of satellite observations, orbital information, and preliminary results of data analyses prior to formal publication in the appropriate journals. The Reports are also used extensively for the rapid publication of preliminary or special results in other fields of astrophysics.

The Reports are regularly distributed to all institutions participating in the U. S. space research program and to individual scientists who request them from the Publications Division, Distribution Section, Smithsonian Astrophysical Observatory, Cambridge, Massachusetts 02138.